Received: 12 August 2024 | Accepted: 10 October 2024

DOI: 10.1111/1751-7915.70038

MICROBIAL BIOTECHNOLOGY Open Access

RESEARCH ARTICLE

Metabolic engineering of *Streptomyces roseosporus* for increased production of clinically important antibiotic daptomycin

Xingwang Li[1] | **Ziwei Sang**[1] | **Xuejin Zhao**[2] | **Ying Wen**[1]

[1]State Key Laboratory of Animal Biotech Breeding and College of Biological Sciences, China Agricultural University, Beijing, China

[2]CAS Key Laboratory of Pathogenic Microbiology and Immunology, Institute of Microbiology, Chinese Academy of Sciences, Beijing, China

Correspondence
Xuejin Zhao, CAS Key Laboratory of Pathogenic Microbiology and Immunology, Institute of Microbiology, Chinese Academy of Sciences, Beijing 100101, China.
Email: zhaoxj@im.ac.cn

Ying Wen, State Key Laboratory of Animal Biotech Breeding and College of Biological Sciences, China Agricultural University, Beijing 100193, China.
Email: wen@cau.edu.cn

Funding information
National Natural Science Foundation of China, Grant/Award Number: 32170081; National Key Research and Development Program of China, Grant/Award Number: 2023YFC3402400

Abstract

Daptomycin (DAP), a novel cyclic lipopeptide antibiotic produced by *Streptomyces roseosporus*, is clinically important for treatment of infections caused by multidrug-resistant Gram-positive pathogens, but the low yield hampers its large-scale industrial production. Here, we describe a combination metabolic engineering strategy for constructing a DAP high-yielding strain. Initially, we enhanced aspartate (Asp) precursor supply in *S. roseosporus* wild-type (WT) strain by separately inhibiting Asp degradation and competitive pathway genes using CRISPRi and overexpressing Asp synthetic pathway genes using strong promoter *kasOp**. The resulting strains all showed increased DAP titre. Combined inhibition of *acsA4*, *pta*, *pyrB*, and *pyrC* increased DAP titre to 167.4 μg/mL (73.5% higher than WT value). Co-overexpression of *aspC*, *gdhA*, *ppc*, and *ecaA* led to DAP titre 168 μg/mL (75.7% higher than WT value). Concurrently, we constructed a chassis strain favourable for DAP production by abolishing by-product production (i.e., deleting a 21.1 kb region of the red pigment biosynthetic gene cluster (BGC)) and engineering the DAP BGC (i.e., replacing its native *dptEp* with *kasOp**). Titre for the resulting chassis strain reached 185.8 μg/mL. Application of our Asp precursor supply strategies to the chassis strain further increased DAP titre to 302 μg/mL (2.1-fold higher than WT value). Subsequently, we cloned the engineered DAP BGC and duplicated it in the chassis strain, leading to DAP titre 274.6 μg/mL. The above strategies, in combination, resulted in maximal DAP titre 350.7 μg/mL (2.6-fold higher than WT value), representing the highest reported DAP titre in shake-flask fermentation. These findings provide an efficient combination strategy for increasing DAP production and can also be readily applied in the overproduction of other Asp-related antibiotics.

INTRODUCTION

The Gram-positive *Streptomyces* species are an industrially important group characterized by the production of a large variety of secondary metabolites such as antibiotics, anticancer drugs, immunosuppressants, and insecticides (Li et al., 2021). Antibiotics are the most important secondary metabolites that display a wide range of biological activities and therapeutic spectra and are widely applied in human medicine, agriculture, and animal husbandry. More than half of the known antibiotics are sourced from *Streptomyces*. In addition, genome sequencing and mining have revealed numerous uncharacterized antibiotic biosynthetic gene clusters (BGCs) in *Streptomyces*, highlighting their valuable potential for producing novel

antibiotics (Blin et al., 2021; Gavriilidou et al., 2022; Lucas et al., 2013). However, large-scale industrial production of antibiotics using *Streptomyces* is generally limited by low yields, as antibiotic biosynthesis is tightly controlled by complex regulatory networks and the precursors of antibiotics are typically generated by primary metabolism, which are also required for cell growth (Cao et al., 2020). Therefore, antibiotic biosynthesis competes with primary metabolic pathways for common precursors and insufficient precursor supply is an obstacle to improving antibiotic production.

In recent years, there has been a growing focus on improving antibiotic production by enhancing precursor supply. Wang et al. (2020) found that intracellular triacylglycerol (TAG) pool can be degraded during stationary growth phase, providing necessary acyl-CoA precursors for polyketide antibiotic biosynthesis. To balance TAG distribution between cell growth and antibiotic biosynthesis, they developed a dynamic degradation of TAG (ddTAG) strategy based on the cumate inducible system to regulate TAG pool, redirecting more carbon flux towards antibiotic biosynthesis without reducing cell growth. Using this strategy, the yields of polyketide antibiotics actinorhodin, oxytetracycline, jadomycin B, and avermectin B1a were significantly increased in four different *Streptomyces* species. An et al. (2021) increased acyl-CoA precursor supply by overexpressing acetyl-CoA carboxylase, propionyl-CoA carboxylase, and acetyl-CoA synthetase genes in heterologous spinosyn-producer *Streptomyces albus* J1074, which led to increased spinosad production. Our laboratory increased acyl-CoA precursor supply by overexpressing *Streptomyces avermitilis* native β-oxidation pathway genes *fadAB* and *fadD*, or/and heterologous cyanobacterial CO_2-concentrating mechanism genes *bicA* and *ecaA* using the native temporal promoter *pkn5p* (active mainly in middle-to-late fermentation stage), thereby increasing avermectin B1a production in an industrial strain (Hao et al., 2022). These findings indicate the importance of enhancing precursor supply for increasing antibiotic production. However, the current precursor supply strategies in *Streptomyces* are mainly focused on enhancing acetyl-CoA precursor supply for polyketide antibiotic production.

Antibiotic BGCs are tightly controlled by multiple levels of transcriptional regulators, resulting in a complex regulatory network (Liu et al., 2013; Urem et al., 2016). However, the regulatory mechanisms involved in antibiotic biosynthesis in *Streptomyces* are insufficiently understood. Thus, promoter engineering offers an efficient strategy for rapid and effective BGC reconstruction by using well-characterized promoters for transcriptional activation or optimization of BGC expression (Bu et al., 2021; Ji et al., 2018, 2022; Zhao et al., 2024). In addition, increasing copy number of BGC is also an effective approach for overexpressing biosynthetic genes, thereby enhancing antibiotic production (Li et al., 2019; Li, Gao, et al., 2022; Li, Pan, et al., 2022). However, there have been no reports on combining promoter engineering and multiple copies of BGC to enhance antibiotic production.

Daptomycin (DAP), produced by *Streptomyces roseosporus*, is a novel calcium-dependent cyclic lipopeptide antibiotic that is clinically important for treatment of infections caused by Gram-positive bacteria, including methicillin-resistant *Staphylococcus aureus* and vancomycin-resistant *Enterococci* (Baltz, 2009; Gonzalez-Ruiz et al., 2016). In addition to DAP, *S. roseosporus* also produces an undesired by-product red pigment, which interferes with isolation and purification process and affects DAP quality. Recently, we identified the BGC responsible for red pigment synthesis in *S. roseosporus* by disrupting the core structural gene *SSIG_RS15030* using a group II intron-based gene editing tool and demonstrated that red pigment synthesis inhibits DAP production (Sang et al., 2024).

DAP is regarded as the best substituent to vancomycin and the last-line of defence against multidrug-resistant Gram-positive pathogens due to its unique mechanism of action and low susceptibility to cross-resistance with other antibiotics (Zuttion et al., 2020). The rapid emergence of multidrug-resistant pathogens worldwide has greatly increased the clinical demand for DAP in recent years. Therefore, there is an urgent need to construct DAP high-yielding strains. Although many efforts have been made to improve DAP yield by traditional random mutagenesis (Yu et al., 2011), optimizing fermentation process (Ng et al., 2014), increasing supply of non-proteinogenic amino acid precursor kynurenine (Kyn) (Liao et al., 2013), increasing resistance to toxic precursor decanoic acid (Lee et al., 2016), engineering regulatory genes (Chen et al., 2022; Huang et al., 2017; Luo et al., 2018; Mao et al., 2015, 2017; Yan et al., 2020; Yuan et al., 2016; Zhang et al., 2015), disrupting biosynthesis of red pigment (Lyu et al., 2022; Sang et al., 2024), and utilizing metabolic engineering (Lyu et al., 2022) and synthetic biology (Ji et al., 2022) approaches, DAP yield remains low. The highest reported DAP titres were only 230 μg/mL in shake-flask culture (Ji et al., 2022) and 812 μg/mL in fed-batch fermentation (Ng et al., 2014).

DAP consists of 13 amino acids with a decanoic acid chain and is synthesized by non-ribosomal peptide synthases (NRPSs) (Robbel & Marahiel, 2010). A cyclic polypeptide of 10 amino acids is formed via an ester bond between Kyn^{13} and $threonine^{4}$ (Thr^{4}), leaving an N-terminal three-amino-acid tail with a decanoic acid moiety attached to $tryptophan^{1}$ (Trp^{1}). Of the 13 amino acids, three are aspartates (Asp^{3}, Asp^{7}, Asp^{9}), suggesting that Asp is the most critical amino acid precursor for DAP biosynthesis. We thus suppose that increase of Asp supply would lead to increased DAP production. However, an effective strategy for increasing

Asp precursor supply in *Streptomyces* has not been documented.

In this study, we enhanced Asp precursor supply in *S. roseosporus* by inhibiting genes involved in Asp degradation and competitive pathways using CRISPRi and overexpressing genes involved in Asp synthetic pathways, thereby increasing DAP production. We also abolished red pigment production by deleting a 21.1 kb region of its BGC and engineered the DAP BGC (termed *dpt* cluster) by promoter engineering. Finally, we cloned and integrated an extra copy of the engineered DAP BGC (termed *dpt** cluster) into *S. roseosporus* chromosome. These multilevel metabolic engineering strategies, in combination, greatly enhanced DAP production (Figure 1). Our strategies described here will be useful for improving the production of other antibiotics using Asp as a precursor.

EXPERIMENTAL PROCEDURES

Strains, plasmids, primers, and growth conditions

Strains and plasmids used in this work are listed in Table S1, and primers in Table S2. *S. roseosporus* strains were cultured as previously described (Yan et al., 2020; Zhang et al., 2015). DA1 agar (Zhang et al., 2015) was used for sporulation and phenotype observation of *S. roseosporus* strains. For DAP production, seed medium (3% Trypticase soy broth, 2.5% dextrin) and fermentation medium (1.1% yeast extract, 0.086% $Fe(NH_4)_2(SO_4)_2{\cdot}6H_2O$, 7.2% dextrin, 1.07% glucose, 1% sucrose) were used.

Escherichia coli strains JM109, EPI300, and ET12567 (Macneil & Klapko, 1987) were cultured in Luria-Bertani (LB) medium for, respectively, routine cloning, cloning of the *dpt** cluster, and propagation of non-methylated plasmids for transformation into *S. roseosporus* strains.

Construction of CRISPRi strains

The CRISPRi plasmids were constructed based on pSET-dcas9 (Zhao et al., 2018) by inserting a 20-nt specific guide sequence (N20) of sgRNA targeting the non-template (NT) strand of gene of interest. The N20 guide sequences of sgRNAs were designed using online software CRISPy-web (http://crispy.secondarymetabolites.org) (Blin et al., 2016) and were synthesized by PCR annealing using primer pairs LXW1A/B~LXW10A/B, respectively, and ligated into *BsaI*-digested pSET-dcas9 (in which *dcas9* and sgRNA were respectively driven by strong constitutive promoters *ermEp** and *j23119p*) to construct CRISPRi plasmids: pdldh^i, pacsA4^i, pacsA1^i, ppta^i, pacyP^i, packA^i, pnadB^i, ppyrB^i, ppyrC^i, and ppoxB^i. These plasmids were separately transformed into protoplasts of *S. roseosporus* wild-type (WT) strain NRRL11379 to generate corresponding strains dldh^i,

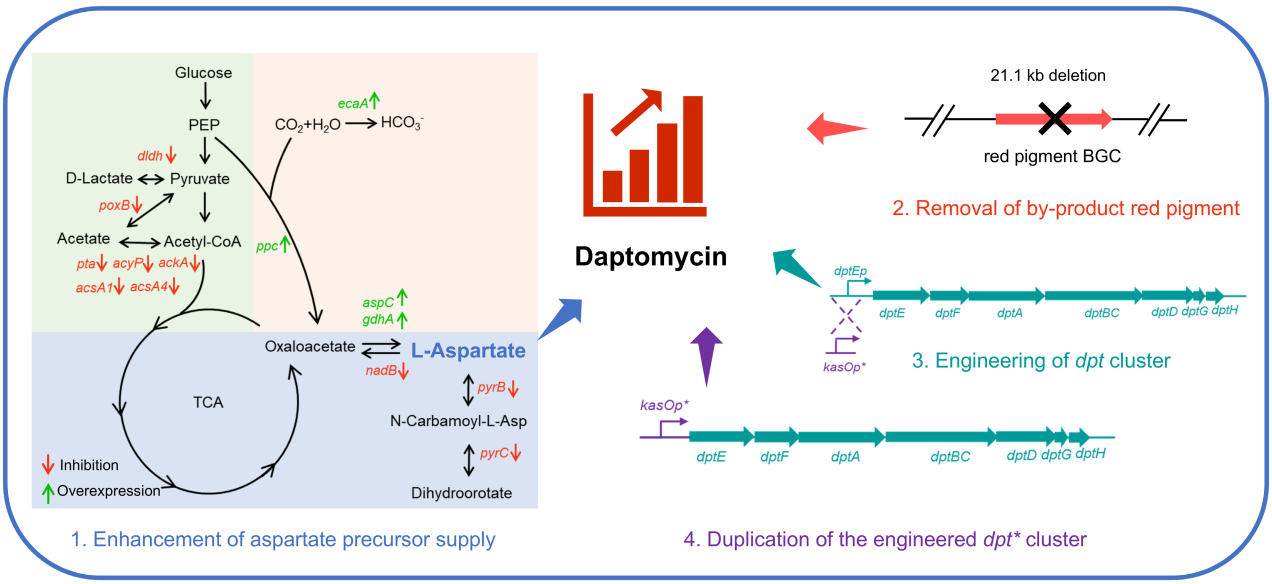

FIGURE 1 Overview of the multilevel metabolic engineering strategies for high DAP production in *S. roseosporus*. Enzymes encoded by genes: *dldh* (*SSIG_RS25800*): D-lactate dehydrogenase; *poxB* (*SSIG_RS04730*): Pyruvate oxidase; *pta* (*SSIG_RS08715*): Phosphate acetyltransferase; *acyP* (*SSIG_RS0234230*): Acylphosphatase; *ackA* (*SSIG_RS08720*): Acetate kinase; *acsA1*, *acsA4* (*SSIG_RS14540*, *SSIG_RS04585*): Acetyl-CoA synthetase; *nadB* (*SSIG_RS18555*): Asp oxidase; *pyrB* (*SSIG_RS28925*): Asp carbamoyltransferase; *pyrC* (*SSIG_RS28930*): Dihydroorotase; *ecaA*: Carbonic anhydrase; *ppc* (*SSIG_RS20110*): Phosphoenolpyruvate carboxylase; *aspC* (*SSIG_RS12365*): Asp aminotransferase; *gdhA* (*SSIG_RS21020*): NADH-specific glutamate dehydrogenase. *dpt* cluster: DAP BGC. *dpt** cluster: The engineered DAP BGC, in which the native *dptEp* was replaced by strong constitutive promoter *kasOp**.

acsA4^{i}, acsA1^{i}, pta^{i}, acyP^{i}, ackA^{i}, nadB^{i}, pyrB^{i}, pyrC^{i}, and poxB^{i}.

For construction of CRISPRi plasmids containing multiple sgRNAs, the cassette *j23119p*-sgRNA^{acsA1}-T0 terminator for targeting *acsA1* was amplified by PCR from pacsA1^{i} using primer pair LXW11A/LXW11B and ligated into *Eco*RV-digested pacsA4^{i} to construct pacsA1^{i}acsA4^{i}. The cassette *j23119p*-sgRNA^{acyP}-T0 terminator was amplified from pacyP^{i} using the same primers and ligated into ppta^{i} to construct pacyP^{i}pta^{i}. The cassette *j23119p*-sgRNA^{ackA}-T0 terminator was amplified from packA^{i}, and ligated into pacyP^{i}pta^{i} to construct packA^{i}acyP^{i}pta^{i}. The cassette *j23119p*-sgRNA^{pyrC}-T0 terminator was amplified from ppyrC^{i} and ligated into ppyrB^{i} to construct ppyrB^{i}pyrC^{i}. The cassette *j23119p*-sgRNA^{pta}-T0 terminator was amplified from ppta^{i}, and ligated into ppyrB^{i}pyrC^{i} to construct ppta^{i}pyrB^{i}pyrC^{i}. The cassette *j23119p*-sgRNA^{acsA4}-T0 terminator was amplified from pacsA4^{i}, and ligated into ppta^{i}pyrB^{i}pyrC^{i} to construct pacsA4^{i}pta^{i}pyrB^{i}pyrC^{i}. Plasmids pacsA1^{i}acsA4^{i}, packA^{i}acyP^{i}pta^{i}, ppyrB^{i}pyrC^{i}, and pacsA4^{i}pta^{i}pyrB^{i}pyrC^{i} were separately transformed into WT strain to generate corresponding strains acsA1^{i}acsA4^{i}, ackA^{i}acyP^{i}pta^{i}, pyrB^{i}pyrC^{i}, and acsA4^{i}pta^{i}pyrB^{i}pyrC^{i}.

Construction of *aspC*, *gdhA*, *ppc*, and *ecaA* overexpression strains

For overexpression of *aspC*, *ppc*, or *gdhA*, DNA fragments *aspC* (1227 bp), *ppc* (2730 bp), and *gdhA* (5016 bp) were PCR amplified from genomic DNA of *S. roseosporus* WT strain using primer pairs LXW13A/LXW13B, LXW14A/LXW14B, and LXW15A/LXW15B, respectively. *Streptomyces* high-efficiency constitutive promoter *kasOp** (stronger than *ermEp**) (Wang et al., 2013) was amplified from pKC-kasOp*-aveC8m (Hao et al., 2022) using primer pair LXW12A/LXW12B. *kasOp** fragment was assembled separately with fragments *aspC*, *ppc*, and *gdhA* by overlap extension PCR using primer pairs LXW12A//LXW13B, LXW12A//LXW14B, and LXW12A/LXW15B. The resulting fragments *kasOp*-aspC*, *kasOp*-ppc*, and *kasOp*-gdhA* were cloned into *Nde*I-digested pIJ10500 (Pullan et al., 2011) to construct plasmids pIJ-kasOp*-aspC, pIJ-kasOp*-ppc, and pIJ-kasOp*-gdhA, which were separately transformed into WT to obtain strains OaspC, Oppc, and OgdhA.

For co-overexpression of *aspC*, *gdhA*, and *ppc*, DNA fragments *kasOp*-aspC* and *kasOp*-ppc* were amplified from pIJ-kasOp*-aspC and pIJ-kasOp*-ppc using primer pairs LXW16A/LXW16B and LXW17A/LXW17B, respectively. Fragment *kasOp*-aspC* was cloned into *Spe*I-digested pIJ-kasOp*-gdhA to construct plasmid pIJ-kasOp*-aspC-gdhA. Fragment *kasOp*-ppc* was cloned into *Spe*I-digested pIJ-kasOp*-aspC-gdhA to construct plasmid pIJ-kasOp*-aspC-gdhA-ppc. Plasmids pIJ-kasOp*-aspC-gdhA and pIJ-kasOp*-aspC-gdhA-ppc were separately transformed into WT to obtain strains OaspC-gdhA and OaspC-gdhA-ppc.

For overexpression of *ecaA*, a 795-bp DNA fragment was amplified from pIJ-pkn5p-ecaA (Hao et al., 2022) using primer pair LXW18A/LXW18B. Promoter *kasOp** was assembled with *ecaA* fragment by overlap extension PCR using primer pairs LXW12A/LXW18B. *kasOp*-ecaA* fragment was cloned into *Spe*I-digested pIJ-kasOp*-aspC-gdhA-ppc to construct plasmid pIJ-kasOp*-aspC-gdhA-ppc-ecaA, which was transformed into WT to obtain strain OaspC-gdhA-ppc-ecaA.

Construction of red pigment BGC deletion strain

The main genes responsible for red pigment biosynthesis extend ~21.1 kb region within its BGC (Figure S1A). To delete this region, homologous recombination strategy was used. Two homologous arms flanking the region were prepared by PCR from WT genomic DNA. A 1074-bp 5′-flanking fragment (positions +1225 to +2298 relative to *SSIG_RS15060* start codon) was amplified using primer pair LXW19A/LXW19B, and a 1026-bp 3′-flanking fragment (positions −139 to +887 relative to *SSIG_RS36015* start codon) was amplified using primer pair LXW20A/LXW20B. The two fragments were ligated by fusion PCR using primer pair LXW19A/LXW20B and cloned into *Nco*I-digested pCIMt005 (Li et al., 2015) to construct deletion vector pΔRED, which was then transformed into WT. The expected mutant, termed ΔRED, was confirmed by PCR using primer pairs LXW21A/LXW21B (flanking the deletion region) and LXW22A/LXW22B (located within the deletion region) (Figure S1B), followed by DNA sequencing. Use of LXW21A/LXW21B generated a 144-bp band in ΔRED, whereas no band was detected in WT. When LXW22A/LXW22B was used, only WT produced a 407-bp band (data not shown).

Construction of strains with replacement of *dptEp* by *kasOp**

To replace promoter *dptEp* in situ with *kasOp**, two fragments flanking *dptEp* were generated by PCR from WT genomic DNA. A 745-bp 5′ flanking region (positions −1121 to −377 relative to *dptE* start codon) was amplified using primer pair LXW23A/LXW23B and a 714-bp 3′ flanking region (positions +1 to +714 relative to *dptE* start codon) was amplified using primer pair LXW25A/LXW25B. *kasOp** fragment was amplified from pKC-kasOp*-aveC8m using primer

pair LXW24A/LXW24B. The three fragments were ligated into *Nco*I-digested pCIMt005 using a seamless assembly cloning kit (Clone Smarter, USA) to construct *dptEp* replacement vector pkasOp*-dptE, which was then transformed into WT. The expected mutant, termed kasOp*-dptE, was confirmed by PCR using primer pairs LXW26A/LXW26B (flanking the exchange regions) (Figure S2), followed by DNA sequencing. Use of LXW26A/LXW26B generated a 2028-bp band in WT and a 1758-bp band in kasOp*-dptE (data not shown).

To delete the 21.1 kb region of red pigment BGC in kasOp*-dptE, the vector pΔRED was transformed into kasOp*-dptE protoplasts. The expected mutant, termed kasOp*-dptE/ΔRED, was isolated by selection of ΔRED and confirmed by PCR using the same primers. Plasmids pacsA4^{i}pta^{i}pyrB^{i}pyrC^{i} and pIJ-kasOp*-aspC-gdhA-ppc-ecaA were separately or co-transformed into kasOp*-dptE/ΔRED to obtain strains XW1, XW2, and XW1-2.

Direct cloning and integration of the engineered *dpt** cluster

Cas9-Assisted Targeting of Chromosome Segments (CATCH) technique (Jiang et al., 2015) was used to capture ~60-kb fragment containing the engineered *dpt** cluster from strain kasOp*-dptE. Briefly, mycelia of kasOp*-dptE were collected from 2-day culture in fermentation medium, and genomic DNA plugs were prepared using the CHEF Bacterial Genomic DNA Plug Kit (Bio-Rad, USA). Two sgRNA sequences (sgRNA-dapF and sgRNA-dapR) were designed for targeting both flanking regions of the *dpt** cluster. The DNA templates of sgRNA-dapF and sgRNA-dapR in vitro transcription were generated by overlapping PCR using three primers: sgRNA-dapF or sgRNA-dapR, guide RNA-F, and guide RNA-R. Then, in vitro transcription of sgRNAs by T7 RNA polymerase was performed using the HiScribe™ T7 Quick High Yield RNA Synthesis Kit (New England Biolabs, USA) according to the manufacturer's protocol. The kasOp*-dptE genomic DNA plug was digested with Cas9, together with sgRNA-dapF and sgRNA-dapR, as previously described (Jiang et al., 2015). The digested DNA was then precipitated with ethanol and suspended in 20 μL DNase-free water. Plasmid pSET156 was constructed from pSET152 (Bierman et al., 1992) by replacing the high copy pUC replicon with the low copy pSC101 replicon of *E. coli*. The linear backbone of pSET156 was amplified from plasmid pSET156 by PCR using primers dap-156-F and dap-156-R, each of which contains a ~30 bp overlap with one end of the target gene cluster fragment. Approximately 50 ng of the backbone DNA and 1 μg of the digested genomic DNA were assembled using Gibson assembly method, and the resulting product was transformed into *E. coli* EPI300 competent cells by electroporation. The correct clones containing recombinant plasmid pSET156-dpt* (Figure S3A) were verified by PCR using primer pairs L-dap yzf /L-dap yzr, R-dap yzf /R-dap yzr, dap1 yzf/dap1 yzr, and dap2 yzf/dap2 yzr (Figure S3B). After isolation, pSET156-dpt* was transferred into kasOp*-dptE/ΔRED by conjugation (Kieser et al., 2000) to obtain strain XW3, which contains an extra copy of the *dpt** cluster.

For combination of Asp precursor supply strategies in strain XW3, ~6 kb DNA fragment containing *dcas9*-sgRNA expression cassette for targeting *acsA4*, *pta*, *pyrB*, and *pyrC* was amplified from pacsA4^{i}pta^{i}pyrB^{i}-pyrC^{i} using primer pair LXW27A/LXW27B and cloned into *Hin*dIII-digested pIJ-kasOp*-aspC-gdhA-ppc-ecaA to construct plasmid pXW1-2, which was then transformed into XW3 to obtain strain XW1-2-3.

Production and analysis of DAP

Fermentation of *S. roseosporus* strains and measurement of DAP yield in fermentation broth by HPLC were performed as previously described (Zhang et al., 2015).

RNA extraction and RT-qPCR analysis

For RNA extraction, *S. roseosporus* strains were cultured in fermentation medium for various times, and mycelia were collected and ground in liquid nitrogen. Total RNA was extracted from mycelia using Trizol reagent (Tiangen, China). Then crude RNA sample was treated with DNase I (TaKaRa, China) to eliminate genomic DNA contamination. Transcription levels of tested genes were determined by RT-qPCR analysis as previously described (Zhang et al., 2015) using corresponding primers listed in Table S2. Relative expression value of each gene was normalized internally to the value of gene reference *hrdB* (*SSIG_RS06665*). Each experiment was conducted in triplicate.

Analysis of intracellular L-Asp

Streptomyces roseosporus mycelia cultured in fermentation medium for various times were ground in liquid nitrogen. The powder was suspended in PBS buffer and sonicated on ice for 5 min. After centrifugation, the supernatant was taken to determine the content of L-Asp using the Amplite™ Fluorimetric L-Asp Assay Kit (AAT Bioquest, USA). Fluorescence intensity was measured by multifunctional microplate reader (SpectraMax i3x, Austria), with an excitation wavelength 540 nm and an emission wavelength 590 nm. L-Asp content was calculated from a standard curve constructed using L-Asp standard provided in the kit.

RESULTS

Exogenous addition of Asp promotes DAP production

Structural analysis of DAP (Figure 2A) suggests that Asp plays a critical role in DAP biosynthesis. To test this, we added different concentrations (30, 60, 90 mg/L) of Asp to fermentation medium of *S. roseosporus* WT strain based on the study of Zhu et al. (2021) and measured DAP titres from 10-day culture by HPLC. The results showed that supplementation of Asp benefited DAP production, and addition of 60 mg/L Asp resulted in the highest titre: 134.8 μg/mL, which was 41.3% higher than the control value (95.4 μg/mL) (Figure 2B). Therefore, insufficient Asp supply might limit DAP production, and enhancement of Asp supply could promote DAP production.

Downregulation of Asp degradation pathway genes promotes DAP production

Although exogenous addition of Asp could promote DAP production, it is uneconomical and inconvenient for scaled-up fermentation. Therefore, we attempted to enhance Asp supply for DAP production by metabolic pathway optimization strategy. Based on the predicted pathways related to Asp synthesis in *S. roseosporus* (Figure 3), Asp can be degraded into dihydroorotate under the catalysis of Asp carbamoyltransferase (encoded by *pyrB*) and dihydroorotase (encoded by *pyrC*). Asp can also be converted to oxaloacetate (OAA) by Asp oxidase (encoded by *nadB*). To investigate the effect of *pyrB*, *pyrC*, and *nadB* on DAP production, we downregulated each of these three genes by CRISPRi. One sgRNA was designed for each gene to target the NT strand of the coding region close to the start codon. Three CRISPRi plasmids ppyrB^{i}, ppyrC^{i}, and pnadB^{i} were accordingly constructed and separately transformed into *S. roseosporus* WT, resulting in CRISPRi strains pyrB^{i}, pyrC^{i}, and nadB^{i}. pSET-dcas9 without 20 nt specific guide sequence of sgRNA was also transformed into WT to obtain plasmid control strain WT/dcas9.

RT-qPCR analysis showed that transcription levels of *pyrB*, *pyrC*, and *nadB* were all lower in the corresponding CRISPRi strains than in WT grown in fermentation medium at both time points day 2 (exponential phase) and day 6 (stationary phase) (Figure S4), indicating successful inhibition of these genes in the CRISPRi strains. HPLC analysis of final DAP titres from 10-day culture revealed that control strain WT/dcas9 showed no significant titre difference from WT, whereas inhibition of *pyrB*, *pyrC*, and *nadB* (strains pyrB^{i}, pyrC^{i}, and nadB^{i}) all resulted in increased DAP titres (Figure 4A). Among the three CRISPRi strains, pyrC^{i} showed the highest DAP titre: 148.4 μg/mL – 53.8% higher than WT value (96.5 μg/mL). pyrB^{i} had the second highest DAP titre: 129.8 μg/mL – 34.5% higher than WT value. nadB^{i} showed only 10.1% increase of DAP titre: 106.2 μg/mL. Simultaneous inhibition of *pyrB* and *pyrC* located in the same branch pathway (strain pyrB^{i}pyrC^{i}) further increased DAP titre to 154.7 μg/mL – 60.3% higher than WT value (Figure 4A). These findings indicate that inhibition of Asp degradation pathway genes is an effective strategy for enhancement of DAP production.

Downregulation of competitive pathway genes for Asp synthesis promotes DAP production

As a key direct precursor of Asp synthesis, intracellular supply of OAA plays a critical role in Asp accumulation

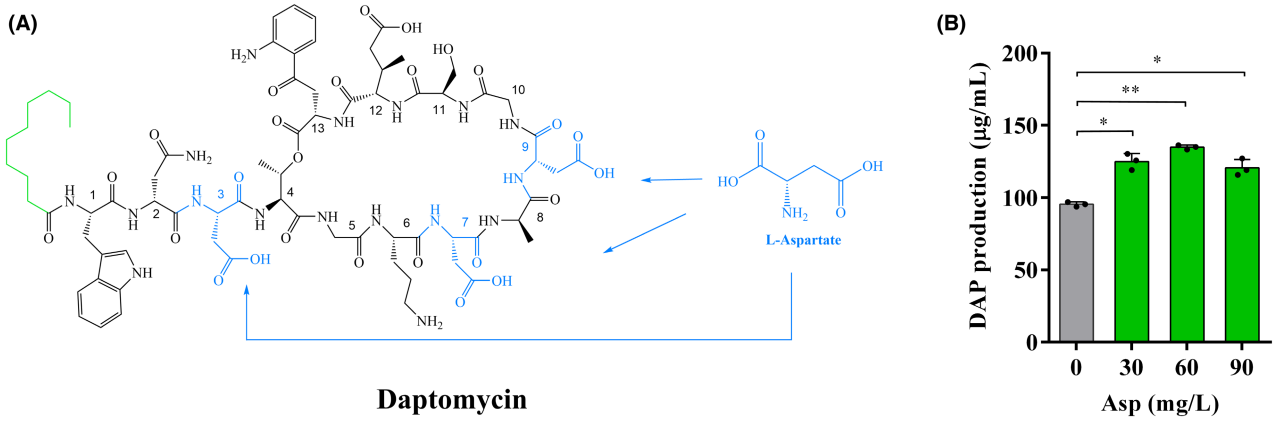

FIGURE 2 Structure of DAP (A) and effect of Asp addition (30, 60, 90 mg/L) on DAP production (B). (A) DAP consists of 13 amino acids and a decanoic acid chain. The amino acids are in the order: Trp[1], D-Asparagine[2] (D-Asn[2]), Asp[3], Thr[4], Glycine[5] (Gly[5]), Ornithine[6] (Orn[6]), Asp[7], D-Alanine[8] (D-Ala[8]), Asp[9], Glycine[10] (Gly[10]), D-Serine[11] (D-Ser[11]), Methylglutamate[12] (MeGlu[12]), Kyn[13]. Blue colour: Asp. Green colour: Decanoic acid chain. (B) *S. roseosporus* WT strain was cultured in fermentation medium for 10 days. No addition of Asp (0 mg/L) was used as control. *$p < 0.05$; **$p < 0.01$ for comparison with control value (Student's *t*-test). Error bars: SD from three replicates.

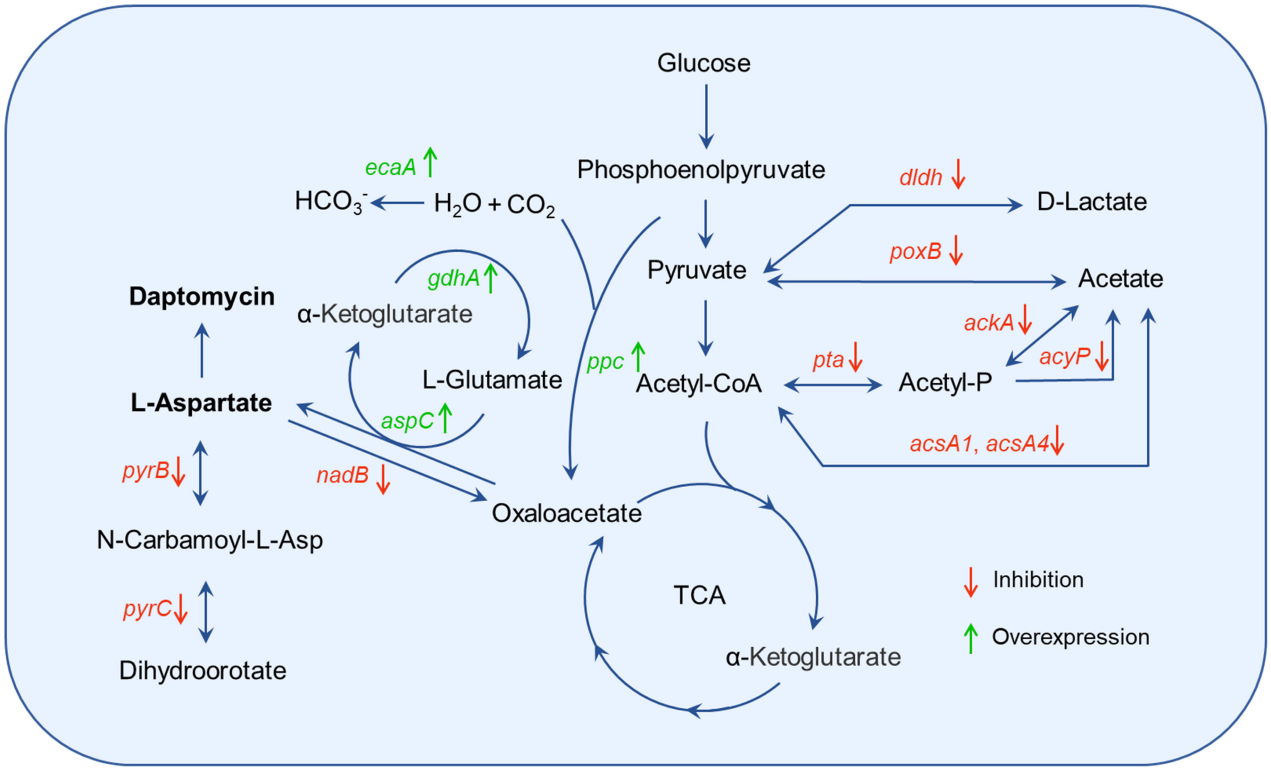

FIGURE 3 Strategies for enhanced Asp precursor supply for improvement of DAP production (schematic). Red colour: Ten genes selected as CRISPRi targets. Green colour: Four genes selected for overexpression.

(Piao et al., 2019; Zhu et al., 2021). OAA is located at the key node of central carbon metabolism pathways involving glycolysis and tricarboxylic acid (TCA) cycle. In *S. roseosporus*, pyruvate (the key precursor of acetyl-CoA) can be converted to by-products D-lactate and acetate by D-lactate dehydrogenase (encoded by *dldh*) and pyruvate oxidase (encoded by *poxB*), respectively; acetyl-CoA (the key precursor of TCA) can be converted to by-product acetate by phosphate acetyltransferase-acetate kinase (encoded by *pta-ackA*), phosphate acetyltransferase-acylphosphatase (encoded by *pta-acyP*), or acetyl-CoA synthetase (encoded by *acsA1* or *acsA4*) (Figure 3). To redirect more carbon flux towards OAA pool and thereby enhance Asp supply for DAP production, we downregulated each of the above seven competitive pathway genes by CRISPRi in *S. roseosporus* WT to obtain strains dldh^{i}, poxB^{i}, pta^{i}, ackA^{i}, acyP^{i}, acsA1^{i}, and acsA4^{i}. Successful inhibition of *dldh*, *poxB*, *pta*, *ackA*, *acyP*, *acsA1*, or *acsA4* in the corresponding CRISPRi strains was demonstrated by RT-qPCR analysis (Figure S5).

Shake-flask fermentation results showed that final DAP titre was increased in all the seven CRISPRi strains (Figure 4B). Strain pta^{i} showed the highest DAP titre: 142.1 μg/mL – 47.3% higher than WT value (96.5 μg/mL). Strain acsA4^{i} had the second highest DAP titre: 121.7 μg/mL – 26.1% higher than WT value. Simultaneous inhibition of *ackA-acyP-pta* or *acsA1-acsA4* located in the same branch pathway further increased DAP titre relative to single inhibition of these genes. Titre for ackA^{i}acyP^{i}pta^{i} was 151 μg/mL – 56.5% higher than WT value and higher than ackA^{i} (112.1 μg/mL), acyP^{i} (113.8 μg/mL), and pta^{i} values. Titre for acsA1^{i}acsA4^{i} was 130.1 μg/mL – 34.8% higher than WT value and higher than acsA1^{i} (111 μg/mL) and acsA4^{i} values (Figure 4B). These findings indicate that inhibition of competitive pathway genes for Asp synthesis effectively enhances DAP production.

Combined inhibition of Asp degradation and competitive pathway genes further promotes DAP production

To further increase DAP production, we attempted to inhibit both Asp degradation and competitive pathway genes in *S. roseosporus* WT. However, simultaneous inhibition of the above ten genes using our CRISPRi system is difficult due to homologous recombination among sgRNA expression cassettes. Therefore, we selected the two best genes, respectively from Asp degradation (i.e., *pyrB* and *pyrC*) and competitive pathways (i.e., *acsA4* and *pta*) for combined inhibition. Final DAP titre for the resulting strain acsA4^{i}pta^{i}pyrB^{i}pyrC^{i} was further increased to 167.4 μg/mL – respectively 73.5%, 28.7%, 10.9%, and 8.2% higher than values for WT, acsA1^{i}acsA4^{i}, ackA^{i}acyP^{i}pta^{i}, and pyrB^{i}pyrC^{i} (Figure 4C). acsA4^{i}pta^{i}pyrB^{i}pyrC^{i} did not display notable phenotypic

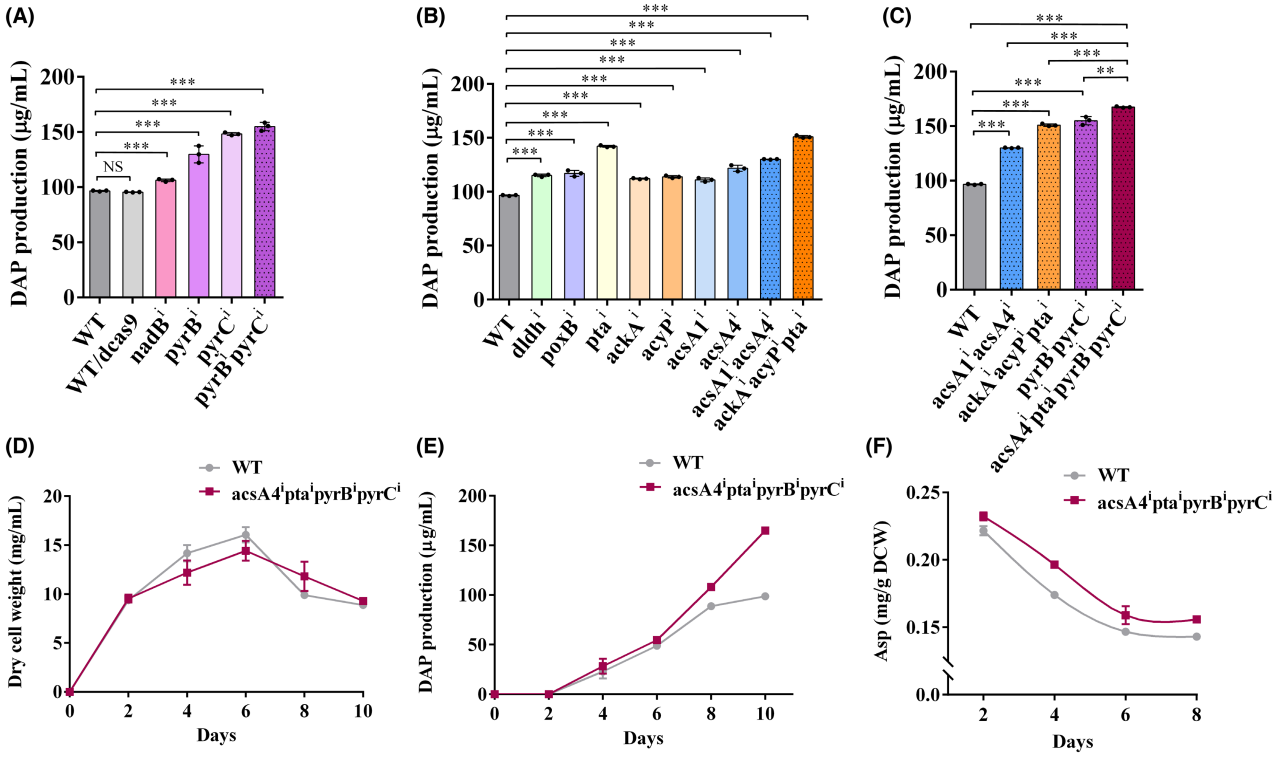

FIGURE 4 Effects of inhibition of Asp degradation and competitive pathway genes on DAP production, cell growth, and Asp level in WT. (A–C) DAP titres for WT and its derived CRISPRi strains on day 10. WT/dcas9: WT with CRISPRi control plasmid pSET-dcas9. (D) Growth curves of WT and acsA4^{i}pta^{i}pyrB^{i}pyrC^i grown in fermentation medium. Biomass is detected as dry cell weight. (E) Time course of DAP titre for WT and acsA4^{i}pta^{i}pyrB^{i}pyrC^i. (F) Asp levels for WT and acsA4^{i}pta^{i}pyrB^{i}pyrC^i on days 2, 4, 6, and 8. Asp level is expressed as mg per g dry cell weight (DCW). NS, not significant; $^{**}p < 0.01$; $^{***}p < 0.001$ (*t*-test). Error bars: SD from three replicates.

difference from WT grown on DA1 plate (Figure S6), and its biomass value (dry cell weight) was comparable to that of WT grown in fermentation medium (Figure 4D), whereas combined inhibition of *acsA4*, *pta*, *pyrB*, and *pyrC* significantly increased DAP titre on days 8 and 10 (Figure 4E).

To investigate whether inhibition of Asp degradation and competitive pathway genes increases Asp supply for DAP production, we measured Asp levels in WT and acsA4^{i}pta^{i}pyrB^{i}pyrC^i cultured in fermentation medium for 2, 4, 6, and 8 days. Asp levels were higher in acsA4^{i}pta^{i}pyrB^{i}pyrC^i than in WT at all four time points (Figure 4F). These findings indicate that inhibition of Asp degradation and competitive pathway genes leads to increased Asp precursor levels, and consequent promotion of DAP production.

Strengthening Asp synthetic pathways promotes DAP production

To further increase Asp supply, we attempted to strengthen Asp synthetic pathways. As shown in Figure 3, Asp can be synthesized directly from OAA under the catalysis of Asp aminotransferase (AspC) using L-glutamate (L-Glu) as an amino group donor. L-Glu dehydrogenase (GDH) catalyses the formation of L-Glu from α-ketoglutarate (α-KG) using NADH/NADPH as cofactor. However, TCA cycle might not produce sufficient α-KG/L-Glu pool to promote AspC-catalysed transamination (Piao et al., 2019). *S. roseosporus* contains NADH-specific GDH gene *gdhA*, which can be used to regenerate L-Glu for AspC and NAD^+ for glycolysis (Figure 5A). Therefore, we overexpressed *aspC* and *gdhA* in WT, respectively, using high-efficiency promoter *kasOp** and integrative plasmid pIJ10500 to strengthen Asp synthesis. Successful overexpression of *aspC* and *gdhA* in the resulting strains OaspC and OgdhA was demonstrated by RT-qPCR analysis (Figure S7). Introduction of control plasmid pIJ10500 (strain WT/pIJ10500) had no effect on DAP production, whereas overexpression of *aspC* and *gdhA* (strains OaspC and OgdhA) both promoted DAP production (Figure 5B). Final DAP titre was 124.3 μg/mL for OaspC (30.0% higher than WT value 95.6 μg/mL) and 124.2 μg/mL for OgdhA (29.9% higher than WT value). Co-overexpression of *aspC* and *gdhA* (strain OaspC-gdhA) further increased DAP titre to 149.1 μg/mL – 56.0% higher than WT value (Figure 5B).

In addition to TCA, OAA (the critical precursor for Asp synthesis) can also be synthesized by carboxylation of pyruvate or phosphoenolpyruvate (PEP). *S. roseosporus* contains PEP carboxylase gene *ppc* (Figures 3 and

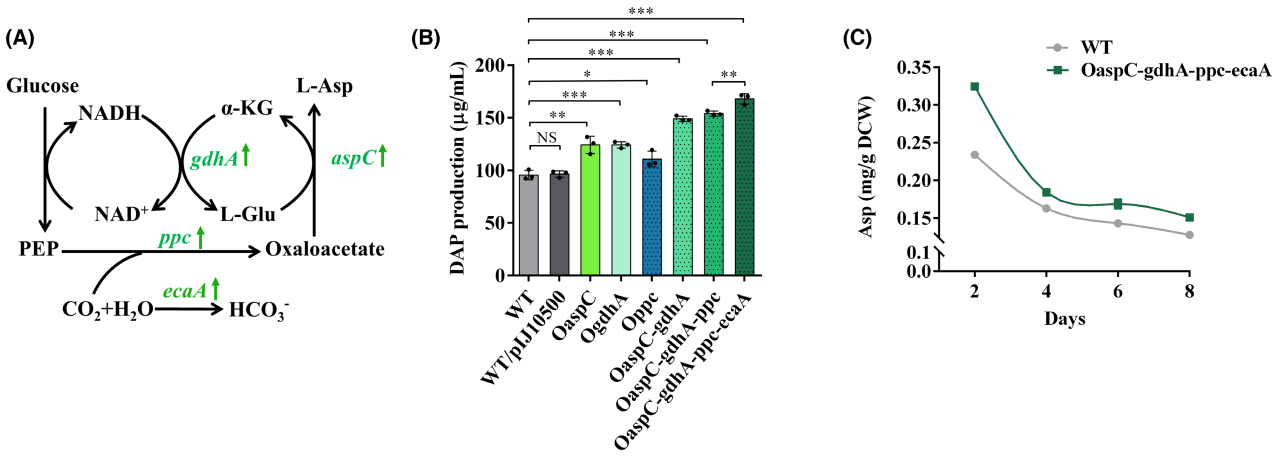

FIGURE 5 Effects of overexpression of Asp synthetic pathway genes on DAP production and Asp level in WT. (A) Schematic of L-Asp formation reaction catalysed by AspC using a cofactor self-sufficient system. NADH-dependent GDH (encoded by *gdhA*) can regenerate L-Glu and NAD^+. PEP carboxylation reaction is catalysed by PEP carboxylase encoded by *ppc*, and carbonic anhydrase (encoded by *ecaA*) converts CO_2 to bicarbonate for activation of PEP carboxylase. (B) DAP titres for WT and its derived overexpression strains on day 10. WT/pIJ10500: WT with control plasmid pIJ10500. NS, not significant; *$p<0.05$; **$p<0.01$; ***$p<0.001$ (*t*-test). (C) Asp levels for WT and OaspC-gdhA-ppc-ecaA on days 2, 4, 6, and 8. Error bars (panels B, C): SD from three replicates.

5A), but not pyruvate carboxylase gene. We therefore overexpressed *kasOp**-driven *ppc* to divert carbon flux from PEP towards OAA and Asp. The resulting strain Oppc displayed DAP titre 110.7 μg/mL – 15.8% higher than WT value (Figure 5B). Co-overexpression of *ppc* with *aspC* and *gdhA* in WT (strain OaspC-gdhA-ppc) further increased DAP titre to 154.1 μg/mL – 61.2% higher than WT value (Figure 5B).

The enzymes responsible for carboxylation reactions generally require bicarbonate and ATP for activation. However, the conversion of intracellular CO_2 to bicarbonate usually has low efficiency, limiting efficient carboxylation reaction. Carbonic anhydrase (encoded by *ecaA*) from *Anabaena sp.* PCC7120 can efficiently catalyse the conversion of CO_2 to bicarbonate (SoltesRak et al., 1997). We previously introduced codon optimized *ecaA* gene into *S. avermitilis* to increase the carboxylation efficiency of acetyl-CoA and propionyl-CoA carboxylases, thereby increasing supply of malonyl- and methylmalonyl-CoA precursors for avermectin production (Hao et al., 2022). To increase the efficiency of PEP carboxylase-catalysed carboxylation reaction, we co-overexpressed *kasOp**-driven codon optimized *ecaA* with *aspC*, *gdhA*, and *ppc* in WT, resulting in strain OaspC-gdhA-ppc-ecaA. Heterologous expression of *ecaA* in OaspC-gdhA-ppc-ecaA was confirmed by RT-qPCR (Figure S7). OaspC-gdhA-ppc-ecaA showed no obvious phenotype and growth changes from WT (Figure S8A,B), but had a final DAP titre 168 μg/mL – respectively 75.7% and 9.0% higher than WT and OaspC-gdhA-ppc values (Figure 5B). Asp level was higher for OaspC-gdhA-ppc-ecaA than for WT (Figure 5C) and contributed to enhanced DAP production.

Construction of a chassis strain favourable for DAP production

To achieve more promoting effect on DAP production by enhancing Asp supply, it is important to construct a suitable chassis strain. Red pigment is the main by-product of *S. roseosporus* that inhibits DAP production (Sang et al., 2024), and its biosynthesis should be abolished. The entire red pigment BGC predicted by antiSMASH software (Blin et al., 2021) is ~72.5 kb, of which the main biosynthetic genes are concentrated in a 21.1 kb region (Figure S1A). To construct a chassis strain for DAP production, we deleted this 21.1 kb region by homologous recombination (Figure 6A and Figure S1B). The resulting strain ΔRED showed a complete loss of red pigment production (Figure 6B), whereas its final DAP titre reached 157.7 μg/mL – 59.8% higher than WT value (98.7 μg/mL) (Figure 6C), confirming our previous finding (Sang et al., 2024).

To further increase DAP production, we next aimed to increase the expression levels of *dpt* genes within DAP BGC (i.e., *dpt* cluster). The *dpt* cluster contains 12 genes, and *dptEp* is the most important promoter in the cluster because it drives the expression of *dptE-dptF-dptA-dptBC-dptD-dptG-dptH* operon (termed *dptE* operon), which contains seven structural genes required for DAP biosynthesis (Figure S2A) (Gal et al., 2006). Transcriptional regulation of *dptEp* is very complex; to date, six transcriptional regulators AtrA (Mao et al., 2015), DepR1 (Yuan et al., 2016), DepR2 (Mao et al., 2017), PhaR (Luo et al., 2018), BldD (Yan et al., 2020), and DasR (Chen et al., 2022) have been identified to target this promoter. To bypass the complex regulation, we replaced the native *dptEp* on *S. roseosporus* WT genome with strong constitutive promoter

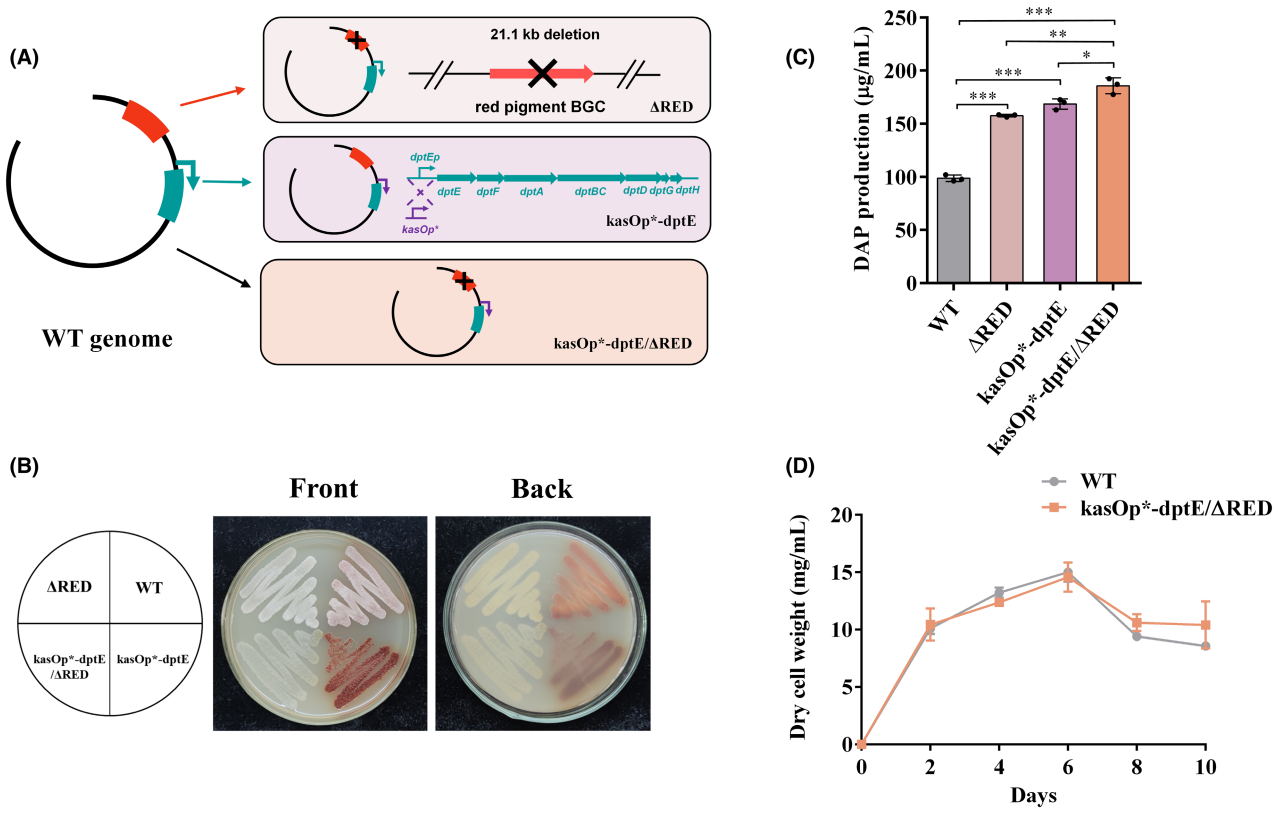

FIGURE 6 Effects of abolishing red pigment production and increasing transcription level of *dptE* operon on phenotype, cell growth, and DAP production in WT. (A) Schematic of construction of strains ΔRED, kasOp*-dptE, and kasOp*-dptE/ΔRED. Red block: Red pigment BGC. Green block: DAP BGC. ΔRED: WT with deleted 21.1 kb region of red pigment BGC. kasOp*-dptE: WT with replacement of *dptEp* by *kasOp**. kasOp*-dptE/ΔRED: kasOp*-dptE with deleted 21.1 kb region of red pigment BGC. (B) Phenotypes of WT, ΔRED, kasOp*-dptE, and kasOp*-dptE/ΔRED grown on DA1 plate for 7 days. (C) DAP titres for the four strains on day 10. *$p < 0.05$; **$p < 0.01$; ***$p < 0.001$ (*t*-test). (D) Growth curves of WT and kasOp*-dptE/ΔRED grown in fermentation medium. Error bars (panels C, D): SD from three replicates.

*kasOp** by homologous recombination (Figure 6A and Figure S2B). The resulting strain kasOp*-dptE produced fewer spores on DA1 plate (Figure 6B), whereas its final DAP titre reached 168.6 μg/mL – 70.8% higher than WT value (Figure 6C). Relative to transcription levels in WT, levels of seven *dpt* genes within *dptE* operon were all upregulated in kasOp*-dptE (Figure S9), accounting for enhanced DAP production. Furthermore, kasOp*-dptE maintained genetic stability after at least five successive passage generations (data not shown).

Although DAP production in kasOp*-dptE was significantly increased, it produced more red pigment than WT with unknown reasons (Figure 6B). Therefore, we also deleted the 21.1 kb region within red pigment BGC in kasOp*-dptE (Figure 6A). As expected, the resulting strain kasOp*-dptE/ΔRED abolished red pigment production (Figure 6B), whereas DAP titre was further increased to 185.8 μg/mL – respectively 88.2%, 17.8%, and 10.2% higher than WT, ΔRED, and kasOp*-dptE values (Figure 6C). Although kasOp*-dptE/ΔRED also produced fewer spores like its parental kasOp*-dptE (Figure 6B), its growth was similar to that of WT (Figure 6D). Thus, kasOp*-dptE/ΔRED can serve as a high-yielding chassis strain for further enhancing DAP production by metabolic engineering or synthetic biology strategies.

Asp precursor supply strategies promote DAP production in chassis strain

In view of the significantly increased DAP production in WT strain achieved using our Asp precursor supply strategies, we applied these strategies in the high-yielding chassis strain kasOp*-dptE/ΔRED. Plasmids pacsA4^{i}pta^{i}pyrB^{i}pyrC^{i} and pIJ-kasOp*-aspC-gdhA-ppc-ecaA were separately transformed into kasOp*-dptE/ΔRED to generate strains XW1 and XW2 (Figure 7A). Final DAP titres for these two strains were 244.5 μg/mL and 248.6 μg/mL – respectively 31.6% and 33.8% higher than the value for parental kasOp*-dptE/ΔRED (Figure 7B). Possible integrative effect was investigated by co-transforming plasmids pacsA4^{i}pta^{i}pyrB^{i}pyrC^{i} and pIJ-kasOp*-aspC-gdhA-ppc-ecaA into kasOp*-dptE/ΔRED. The resulting strain XW1-2 had final DAP titre 302 μg/mL – respectively 62.5% and 2.1-fold higher than kasOp*-dptE/ΔRED and WT values, whereas co-transformation of control

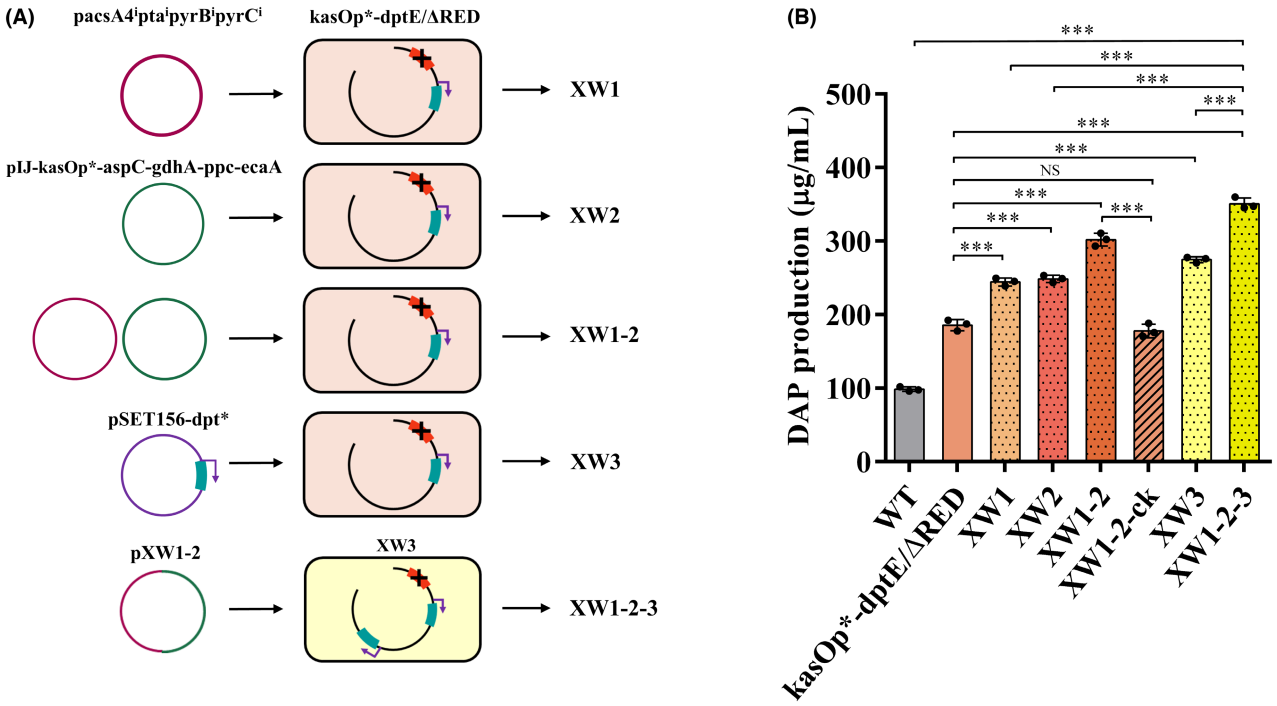

FIGURE 7 Effects of combination of Asp precursor supply strategies and the *dpt** cluster duplication on DAP production in the chassis strain kasOp*-dptE/ΔRED. (A) Schematic of construction of strains XW1, XW2, XW1-2, XW3, and XW1-2-3. XW1: kasOp*-dptE/ΔRED with plasmid pacsA4^{i}pta^{i}pyrB^{i}pyrC^{i}. XW2: kasOp*-dptE/ΔRED with plasmid pIJ-kasOp*-aspC-gdhA-ppc-ecaA. XW1-2: kasOp*-dptE/ΔRED with plasmids pacsA4^{i}pta^{i}pyrB^{i}pyrC^{i} and pIJ-kasOp*-aspC-gdhA-ppc-ecaA. XW3: kasOp*-dptE/ΔRED with an extra copy of the *dpt** cluster. XW1-2-3: XW3 with plasmid pXW1-2. (B) DAP titres for WT, kasOp*-dptE/ΔRED, XW1, XW2, XW1-2, XW1-2-ck, XW3, and XW1-2-3 on day 10. XW1-2-ck: kasOp*-dptE/ΔRED with control plasmids pSET-dcas9 and pIJ10500. NS, not significant; ***$p < 0.001$ (*t*-test). Error bars: SD from three replicates.

plasmids pSET-dcas9 and pIJ10500 into kasOp*-dptE/ΔRED (strain XW1-2-ck) had no effect on DAP titre (Figure 7B). Thus, our Asp precursor supply strategies effectively enhance DAP production in both WT and high-yielding strains.

Introduction of an extra copy of the engineered *dpt** cluster further promotes production

Increasing copy number of BGC is an effective strategy for improving antibiotic production (Li, Gao, et al., 2022; Li, Pan, et al., 2022). As in situ replacement of *dptEp* with *kasOp** increased expression of seven core *dpt* genes and thereby increased DAP production, we directly cloned this engineered *dpt** cluster from strain kasOp*-dptE into integrative plasmid pSET156 to construct pSET156-dpt* (Figure S3), which was then transferred into the chassis strain kasOp*-dptE/ΔRED by conjugation (Figure 7A). DAP titre for the resulting strain XW3 was further increased to 274.6 μg/mL – 47.8% higher than the value for parental kasOp*-dptE/ΔRED (Figure 7B).

Finally, we attempted to combine Asp precursor supply strategies in strain XW3. Because CRISPRi plasmid pacsA4^{i}pta^{i}pyrB^{i}pyrC^{i} and pSET156-dpt* both contain apramycin resistance gene *aac(3)IV* and φC31 integrase gene, it was not possible to transform pacsA4^{i}pta^{i}pyrB^{i}pyrC^{i} into strain XW3. We therefore amplified dcas9-sgRNA expression cassette for targeting *acsA4*, *pta*, *pyrB*, and *pyrC* from pacsA4^{i}pta^{i}pyrB^{i}pyrC^{i} and ligated it into plasmid pIJ-kasOp*-gdhA-aspC-ppc-ecaA to construct pXW1-2, which was then transformed into XW3. The resulting strain XW1-2-3 was similar to WT in terms of cell growth (Figure S10) but had a final DAP titre 350.7 μg/mL – respectively 2.6-fold, 43.4%, 41.1%, and 27.7% higher than values for WT, XW1, XW2, and XW3 (Figure 7B).

DISCUSSION

As secondary metabolites, antibiotics are generally synthesized during stationary phase of *Streptomyces* fermentation, but their precursors (e.g., amino acids, acyl-CoAs) are generated by primary metabolism (which declines in stationary phase) and are also essential building blocks for cell growth. Therefore, it is necessary to optimize precursor supply for increasing antibiotic production (Bu et al., 2021; Li et al., 2021). Asp is the most important precursor for DAP biosynthesis. In the present study, we enhanced Asp precursor supply by inhibiting Asp degradation and

competitive pathway genes and overexpressing Asp synthetic pathway genes, thereby significantly increasing DAP titre in *S. roseosporus* WT and high-yielding strains. Our Asp precursor supply strategies effectively enhanced Asp level and are presumably applicable in other *Streptomyces* species that require Asp precursor for antibiotic production.

The ten CRISPRi strains with a single targeted gene involved in Asp degradation or competitive pathway all showed increased DAP titre relative to WT value, and DAP production was more strongly promoted by simultaneous inhibition of *pyrB*, *pyrC*, *acsA4*, and *pta*. We selected only four genes for combined inhibition due to potential homologous recombination between sgRNA expression cassettes. Recently, Whitford et al. (2023) developed a scalable multiplexed CRISPR-base editing system in *Streptomyces*. Using this system, multiple sgRNAs were co-transcribed from a single promoter and processed by Csy4 (the type I-F CRISPR-associated endoribonuclease) to achieve simultaneous base editing of up to 17 target sites in model species *Streptomyces coelicolor*. Based on these findings, Csy4-mediated processing of sgRNAs may also be used in CRISPRi system to achieve simultaneous inhibition of more than ten genes and further increase DAP production in *S. roseosporus*.

As Asp is an intermediate product of diverse metabolic reactions, it is difficult to maximize metabolic flux for Asp production and identify key bottleneck for Asp accumulation. Besides the ten targets we inhibited, previous studies showed that deletion of Asp catabolism pathway gene *aspA* (encoding Asp ammonia-lyase responsible for the conversion of Asp to fumarate) increased Asp level in *E. coli* (Piao et al., 2019) and *Bacillus licheniformis* (Zhu et al., 2021). *S. roseosporus* genome doesn't contain *aspA* gene, but the predicted KEGG pathway suggests that Asp may be converted to fumarate by adenylosuccinate synthase-adenylosuccinate lyase (encoded by *purA-purB*) or argininosuccinate synthase-argininosuccinate lyase (encoded by *aroG-argH*). These genes will be inhibited with CRISPRi in future studies to investigate their effects on Asp supply and DAP production.

We used two approaches to enhance Asp synthesis for DAP production in *S. roseosporus*: (i) strengthening Asp formation from OAA; (ii) increasing OAA supply. There are two kinds of enzymes responsible for the formation of Asp from OAA: AspC and Asp dehydrogenase (AspDH). Because *S. roseosporus* doesn't have *aspDH* gene, we overexpressed native *aspC* to enhance Asp synthesis. We also overexpressed native GDH gene *gdhA* to simultaneously regenerate L-Glu for AspC and NAD^+ for glycolysis. Co-overexpression of *aspC* and *gdhA* had stronger enhancing effect on DAP titre than separate overexpression of these two genes, indicating that AspC coupled with this cofactor self-sufficient system could efficiently drive Asp formation. AspDH is a rare amino acid dehydrogenase that directly uses ammonia as amino donor. AspDH from *Pseudomonas aeruginosa* could use both NADH and NADPH as cofactors (Li et al., 2011). Heterologous overexpression of *aspDH* in *B. licheniformis* contributed to Asp accumulation and therefore benefited synthesis of target product bacitracin (Zhu et al., 2021). Heterologous expression of *aspDH* in *S. roseosporus* may further enhance Asp supply and DAP production. As for the second approach, we didn't find pyruvate carboxylase gene in *S. roseosporus* and therefore overexpressed native PEP carboxylase gene *ppc* to increase OAA supply and heterologous carbonic anhydrase gene *ecaA* to increase the carboxylation efficiency of PEP carboxylase. *S. coelicolor* contains pyruvate carboxylase gene *pyc*. Heterologous overexpression of *S. coelicolor pyc* in *S. roseosporus* will be conducted in the future to compare its promoting effect on DAP production with native *ppc* overexpression.

During *S. roseosporus* fermentation, production of DAP accompanies with generation of a considerable amount of visible red pigment. Biosynthesis of DAP and red pigment may compete for energy and common precursors. Therefore, abolishment of red pigment biosynthesis resulted in greatly increased DAP titre. In addition to DAP and red pigment BGCs, *S. roseosporus* genome contains 29 other secondary metabolite BGCs and 11 of predicted products belong to NRPS or NRPS-like types (Sang et al., 2024), which may compete for precursors and/or energy with DAP pathway. Thus, deletion of these 11 BGCs may further increase DAP production.

Antibiotic production usually correlates with the transcription levels of its biosynthetic genes (Ji et al., 2022). To increase the expression level of *dpt* cluster, we replaced native *dptEp* with strong constitutive promoter *kasOp** in WT and red pigment BGC deletion mutant ΔRED, which increased DAP titre in both the resulting strains. However, *kasOp** may not be optimal for DAP production and DAP titre may be further increased by stronger constitutive promoters such as *stnYp* (Guo et al., 2023) or certain strong native temporal promoters. We have cloned the engineered *dpt** cluster into *E. coli-Streptomyces* shuttle vector pSET156, thereby enabling easy promoter replacement in vitro using established CATCH method (Jiang et al., 2015; Wei et al., 2022).

We also increased DAP titre by introducing an extra copy of the engineered *dpt** cluster, suggesting that multicopy BGC can efficiently enhance DAP production. Multicopy antibiotic BGC can be achieved by ZouA-mediated tandem amplification system and

integrase-mediated site-specific recombination system. ZouA system could increase BGC copy number to 4–12 and thus successfully enhance production of actinorhodin (Murakami et al., 2011), validamycin A (Zhou et al., 2014), bleomycin (Li, Gao, et al., 2022), and spinosad (Li, Pan, et al., 2022). Based on integrase-mediated site-specific recombination system, Li et al. (2019) developed an advanced multiplex site-specific genome engineering (aMSGE) toolkit allowing for integration of 1–4 extra copies of antibiotic BGCs into *Streptomyces* genomes. Application of these two systems will achieve the possible copy number of the engineered *dpt* cluster with optimal promoter for the maximized DAP production.

In summary, we obtained maximal DAP titre 350.7 μg/mL (2.6-fold higher than WT value) by a combination strategy involving enhancement of Asp precursor supply, removal of by-product red pigment synthesis, engineering of *dpt* cluster by promoter replacement, and duplication of the engineered *dpt** cluster. Our work contributes strategies to titre improvement of other Asp-related antibiotics.

AUTHOR CONTRIBUTIONS

Xingwang Li: Data curation; formal analysis; investigation; validation; visualization; writing – original draft. **Ziwei Sang:** Data curation; investigation; formal analysis; validation. **Xuejin Zhao:** Conceptualization; supervision; writing – review and editing. **Ying Wen:** Conceptualization; funding acquisition; supervision; resources; writing – original draft; writing – review and editing.

ACKNOWLEDGEMENTS

This study was supported by the National Key Research and Development Program of China (Grant No. 2023YFC3402400) and the National Natural Science Foundation of China (Grant No. 32170081).

CONFLICT OF INTEREST STATEMENT

The authors declare that they have no competing interests.

DATA AVAILABILITY STATEMENT

The data that supports the findings of this study are available in the supplementary material of this article.

ORCID

Ying Wen https://orcid.org/0000-0001-8455-6900

REFERENCES

An, Z., Tao, H., Wang, Y., Xia, B., Zou, Y., Fu, S. et al. (2021) Increasing the heterologous production of spinosad in *Streptomyces albus* J1074 by regulating biosynthesis of its polyketide skeleton. *Synthetic and Systems Biotechnology*, 6, 292–301.

Baltz, R.H. (2009) Daptomycin: mechanisms of action and resistance, and biosynthetic engineering. *Current Opinion in Chemical Biology*, 13, 144–151.

Bierman, M., Logan, R., O'Brien, K., Seno, E.T., Rao, R.N. & Schoner, B.E. (1992) Plasmid cloning vectors for the conjugal transfer of DNA from *Escherichia coli* to *Streptomyces* spp. *Gene*, 116, 43–49.

Blin, K., Pedersen, L.E., Weber, T. & Lee, S.Y. (2016) CRISPy-web: an online resource to design sgRNAs for CRISPR applications. *Synthetic and Systems Biotechnology*, 1, 118–121.

Blin, K., Shaw, S., Kloosterman, A.M., Charlop-Powers, Z., van Wezel, G.P., Medema, M.H. et al. (2021) antiSMASH 6.0: improving cluster detection and comparison capabilities. *Nucleic Acids Research*, 49, W29–W35.

Bu, Q.T., Li, Y.P., Xie, H., Li, J.F., Lv, Z.Y., Su, Y.T. et al. (2021) Rational engineering strategies for achieving high-yield, high-quality and high-stability of natural product production in actinomycetes. *Metabolic Engineering*, 67, 198–215.

Cao, Z., Yu, J., Wang, W., Lu, H., Xia, X., Xu, H. et al. (2020) Multi-scale data-driven engineering for biosynthetic titer improvement. *Current Opinion in Biotechnology*, 65, 205–212.

Chen, Q., Zhu, J.Y., Li, X.W. & Wen, Y. (2022) Transcriptional regulator DasR represses daptomycin production through both direct and cascade mechanisms in *Streptomyces roseosporus*. *Antibiotics (Basel)*, 11, 1065.

Gal, M.C., Thurston, L., Rich, P., Miao, V. & Baltz, R.H. (2006) Complementation of daptomycin *dptA* and *dptD* deletion mutations in trans and production of hybrid lipopeptide antibiotics. *Microbiology (Reading)*, 152, 2993–3001.

Gavriilidou, A., Kautsar, S.A., Zaburannyi, N., Krug, D., Muller, R., Medema, M.H. et al. (2022) Compendium of specialized metabolite biosynthetic diversity encoded in bacterial genomes. *Nature Microbiology*, 7, 726–735.

Gonzalez-Ruiz, A., Seaton, R.A. & Hamed, K. (2016) Daptomycin: an evidence-based review of its role in the treatment of gram-positive infections. *Infection and Drug Resistance*, 9, 47–58.

Guo, W., Xiao, Z., Huang, T., Zhang, K., Pan, H.X., Tang, G.L. et al. (2023) Identification and characterization of a strong constitutive promoter *stnYp* for activating biosynthetic genes and producing natural products in *Streptomyces*. *Microbial Cell Factories*, 22, 127.

Hao, Y., You, Y., Chen, Z., Li, J., Liu, G. & Wen, Y. (2022) Avermectin B1a production in *Streptomyces avermitilis* is enhanced by engineering *aveC* and precursor supply genes. *Applied Microbiology and Biotechnology*, 106, 2191–2205.

Huang, X., Ma, T., Tian, J., Shen, L., Zuo, H., Hu, C. et al. (2017) *wblA*, a pleiotropic regulatory gene modulating morphogenesis and daptomycin production in *Streptomyces roseosporus*. *Journal of Applied Microbiology*, 123, 669–677.

Ji, C.H., Kim, H., Je, H.W., Kwon, H., Lee, D. & Kang, H.S. (2022) Top-down synthetic biology approach for titer improvement of clinically important antibiotic daptomycin in *Streptomyces roseosporus*. *Metabolic Engineering*, 69, 40–49.

Ji, C.H., Kim, J.P. & Kang, H.S. (2018) Library of synthetic *Streptomyces* regulatory sequences for use in promoter engineering of natural product biosynthetic gene clusters. *ACS Synthetic Biology*, 7, 1946–1955.

Jiang, W., Zhao, X., Gabrieli, T., Lou, C., Ebenstein, Y. & Zhu, T.F. (2015) Cas9-assisted targeting of chromosome segments CATCH enables one-step targeted cloning of large gene clusters. *Nature Communications*, 6, 8101.

Kieser, T., Bibb, M.J., Chater, K.F., Butter, M.J., Hopwood, D.A. & Bittner, M. (2000) *Practical Streptomyces genetics: a laboratory manual*. Norwich, UK: John Innes Foundation.

Lee, S.K., Kim, H.R., Jin, Y.Y., Yang, S.H. & Suh, J.W. (2016) Improvement of daptomycin production via increased resistance to decanoic acid in *Streptomyces roseosporus*. *Journal of Bioscience and Bioengineering*, 122, 427–433.

Li, H., Gao, W.Y., Cui, Y.F., Pan, Y.Y. & Liu, G. (2022) Remarkable enhancement of bleomycin production through precise

amplification of its biosynthetic gene cluster in *Streptomyces verticillus*. *Science China- Life Sciences*, 65, 1248–1256.
Li, H., Pan, Y.Y. & Liu, G. (2022) Multiplying the heterologous production of spinosad through tandem amplification of its biosynthetic gene cluster in *Streptomyces coelicolor*. *Microbial Biotechnology*, 15, 1550–1560.
Li, L., Wei, K., Liu, X., Wu, Y., Zheng, G., Chen, S. et al. (2019) aMSGE: advanced multiplex site-specific genome engineering with orthogonal modular recombinases in actinomycetes. *Metabolic Engineering*, 52, 153–167.
Li, P.W., Li, J.N., Guo, Z.Y., Tang, W., Han, J.S., Meng, X.X. et al. (2015) An efficient blue-white screening based gene inactivation system for *Streptomyces*. *Applied Microbiology and Biotechnology*, 99, 1923–1933.
Li, S., Li, Z., Pang, S., Xiang, W. & Wang, W. (2021) Coordinating precursor supply for pharmaceutical polyketide production in *Streptomyces*. *Current Opinion in Biotechnology*, 69, 26–34.
Li, Y.X., Kawakami, N., Ogola, H.J.O., Ashida, H., Ishikawa, T., Shibata, H. et al. (2011) A novel L-aspartate dehydrogenase from the mesophilic bacterium PAO1: molecular characterization and application for L-aspartate production. *Applied Microbiology and Biotechnology*, 90, 1953–1962.
Liao, G., Wang, L., Liu, Q., Guan, F., Huang, Y. & Hu, C. (2013) Manipulation of kynurenine pathway for enhanced daptomycin production in *Streptomyces roseosporus*. *Biotechnology Progress*, 29, 847–852.
Liu, G., Chater, K.F., Chandra, G., Niu, G.Q. & Tan, H.R. (2013) Molecular regulation of antibiotic biosynthesis in *Streptomyces*. *Microbiology and Molecular Biology Reviews*, 77, 112–143.
Lucas, X., Senger, C., Erxleben, A., Gruning, B.A., Doring, K., Mosch, J. et al. (2013) StreptomeDB: a resource for natural compounds isolated from *Streptomyces* species. *Nucleic Acids Research*, 41, D1130–D1136.
Luo, S., Chen, X.A., Mao, X.M. & Li, Y.Q. (2018) Transposon-based identification of a negative regulator for the antibiotic hyper-production in *Streptomyces*. *Applied Microbiology and Biotechnology*, 102, 6581–6592.
Lyu, Z.Y., Bu, Q.T., Fang, J.L., Zhu, C.Y., Xu, W.F., Ma, L. et al. (2022) Improving the yield and quality of daptomycin in *Streptomyces roseosporus* by multilevel metabolic engineering. *Frontiers in Microbiology*, 13, 872397.
Macneil, D.J. & Klapko, L.M. (1987) Transformation of *Streptomyce avermitilis* by plasmid DNA. *Journal of Industrial Microbiology & Biotechnology*, 2, 209–218.
Mao, X.M., Luo, S. & Li, Y.Q. (2017) Negative regulation of daptomycin production by DepR2, an ArsR-family transcriptional factor. *Journal of Industrial Microbiology & Biotechnology*, 44, 1653–1658.
Mao, X.M., Luo, S., Zhou, R.C., Wang, F., Yu, P., Sun, N. et al. (2015) Transcriptional regulation of the daptomycin gene cluster in *Streptomyces roseosporus* by an autoregulator, AtrA. *Journal of Biological Chemistry*, 290, 7992–8001.
Murakami, T., Burian, J., Yanai, K., Bibb, M.J. & Thompson, C.J. (2011) A system for the targeted amplification of bacterial gene clusters multiplies antibiotic yield in *Streptomyces coelicolor*. *Proceedings of the National Academy of Sciences of the United States of America*, 108, 16020–16025.
Ng, I.S., Ye, C., Zhang, Z., Lu, Y. & Jing, K. (2014) Daptomycin antibiotic production processes in fed-batch fermentation by *Streptomyces roseosporus* NRRL11379 with precursor effect and medium optimization. *Bioprocess and Biosystems Engineering*, 37, 415–423.
Piao, X., Wang, L., Lin, B., Chen, H., Liu, W. & Tao, Y. (2019) Metabolic engineering of *Escherichia coli* for production of L-aspartate and its derivative beta-alanine with high stoichiometric yield. *Metabolic Engineering*, 54, 244–254.
Pullan, S.T., Chandra, G., Bibb, M.J. & Merrick, M. (2011) Genome-wide analysis of the role of GlnR in *Streptomyces venezuelae* provides new insights into global nitrogen regulation in actinomycetes. *BMC Genomics*, 12, 175.
Robbel, L. & Marahiel, M.A. (2010) Daptomycin, a bacterial lipopeptide synthesized by a nonribosomal machinery. *Journal of Biological Chemistry*, 285, 27501–27508.
Sang, Z., Li, X., Yan, H., Wang, W. & Wen, Y. (2024) Development of a group II intron-based genetic manipulation tool for *Streptomyces*. *Microbial Biotechnology*, 17, e14472.
SoltesRak, E., Mulligan, M.E. & Coleman, J.R. (1997) Identification and characterization of a gene encoding a vertebrate-type carbonic anhydrase in cyanobacteria. *Journal of Bacteriology*, 179, 769–774.
Urem, M., Swiatek-Polatynska, M.A., Rigali, S. & van Wezel, G.P. (2016) Intertwining nutrient-sensory networks and the control of antibiotic production in *Streptomyces*. *Molecular Microbiology*, 102, 183–195.
Wang, W., Li, S., Li, Z., Zhang, J., Fan, K., Tan, G. et al. (2020) Harnessing the intracellular triacylglycerols for titer improvement of polyketides in *Streptomyces*. *Nature Biotechnology*, 38, 76–83.
Wang, W., Li, X., Wang, J., Xiang, S., Feng, X. & Yang, K. (2013) An engineered strong promoter for *streptomycetes*. *Applied and Environmental Microbiology*, 79, 4484–4492.
Wei, W., Wang, W., Li, C., Tang, Y., Guo, Z. & Chen, Y. (2022) Construction and heterologous expression of the di-AFN a(1) biosynthetic gene cluster in *Streptomyces* model strains. *Chinese Journal of Natural Medicines*, 20, 873–880.
Whitford, C.M., Gren, T., Palazzotto, E., Lee, S.Y., Tong, Y.J. & Weber, T. (2023) Systems analysis of highly multiplexed CRISPR-base editing in *Streptomycetes*. *ACS Synthetic Biology*, 12, 2353–2366.
Yan, H., Lu, X.R., Sun, D., Zhuang, S., Chen, Q., Chen, Z. et al. (2020) BldD, a master developmental repressor, activates antibiotic production in two *Streptomyces* species. *Molecular Microbiology*, 113, 123–142.
Yu, G.H., Jia, X.Q., Wen, J.P., Lu, W.Y., Wang, G.Y., Caiyin, Q. et al. (2011) Strain improvement of *Streptomyces roseosporus* for daptomycin production by rational screening of He-Ne laser and NTG induced mutants and kinetic modeling. *Applied Biochemistry and Biotechnology*, 163, 729–743.
Yuan, P.H., Zhou, R.C., Chen, X., Luo, S., Wang, F., Mao, X.M. et al. (2016) DepR1, a TetR family transcriptional regulator, positively regulates daptomycin production in an industrial producer, *Streptomyces roseosporus* SW0702. *Applied and Environmental Microbiology*, 82, 1898–1905.
Zhang, Q.L., Chen, Q., Zhuang, S., Chen, Z., Wen, Y. & Li, J.L. (2015) A MarR family transcriptional regulator, DptR3, activates daptomycin biosynthesis and morphological differentiation in *Streptomyces roseosporus*. *Applied and Environmental Microbiology*, 81, 3753–3765.
Zhao, X.J., Zong, Y.Q., Lou, Q.L., Qin, C.R. & Lou, C.B. (2024) A flexible, modular and versatile functional part assembly toolkit for gene cluster engineering in *Streptomyces*. *Synthetic and Systems Biotechnology*, 9, 69–77.
Zhao, Y.W., Li, L., Zheng, G.S., Jiang, W.H., Deng, Z.X., Wang, Z.J. et al. (2018) CRISPR/dCas9-mediated multiplex gene repression in *Streptomyces*. *Biotechnology Journal*, 13, e1800121.
Zhou, T.C., Kim, B.G. & Zhong, J.J. (2014) Enhanced production of validamycin a in *Streptomyces hygroscopicus* 5008 by engineering validamycin biosynthetic gene cluster. *Applied Microbiology and Biotechnology*, 98, 7911–7922.

Zhu, J., Li, L., Wu, F., Wu, Y., Wang, Z., Chen, X. et al. (2021) Metabolic engineering of aspartic acid supply modules for enhanced production of bacitracin in *Bacillus licheniformis*. *ACS Synthetic Biology*, 10, 2243–2251.

Zuttion, F., Colom, A., Matile, S., Farago, D., Pompeo, F., Kokavecz, J. et al. (2020) High-speed atomic force microscopy highlights new molecular mechanism of daptomycin action. *Nature Communications*, 11, 6312.

SUPPORTING INFORMATION

Additional supporting information can be found online in the Supporting Information section at the end of this article.

How to cite this article: Li, X., Sang, Z., Zhao, X. & Wen, Y. (2024) Metabolic engineering of *Streptomyces roseosporus* for increased production of clinically important antibiotic daptomycin. *Microbial Biotechnology*, 17, e70038. Available from: https://doi.org/10.1111/1751-7915.70038